INTERNATIONAL JOURNAL OF CLIMATOLOGY
Int. J. Climatol. **31**: 415–430 (2011)
Published online 8 January 2010 in Wiley Online Library
(wileyonlinelibrary.com) DOI: 10.1002/joc.2075

Impact of climate change on surface winds in France using a statistical-dynamical downscaling method with mesoscale modelling

Julien Najac,[a] Christine Lac[b] and Laurent Terray[a]*
[a] *Climate Modelling and Global Change Team, CERFACS/CNRS, SUC URA 1875, 42 Avenue Gaspard Coriolis, 31057, Toulouse Cedex 1, France*
[b] *CNRM/GMME/Meso-NH, 42 Avenue Gaspard Coriolis, 31057 Toulouse, France*

ABSTRACT: A statistical-dynamical downscaling method is presented to estimate 10 m wind speed and direction distributions at high spatial resolutions using a weather type based approach combined with a mesoscale model. Daily 850 hPa wind fields (predictors) from ERA40 reanalysis and daily 10 m wind speeds and directions (predictands) measured at 78 meteorological stations over France are used to build and validate the downscaling algorithm over the period 1974–2002. First of all, the daily 850 hPa wind fields are classified into a large number of wind classes and one day is randomly chosen inside each wind class. Simulations with a non-hydrostatic mesoscale atmospheric model are then performed for the selected days over three interactively nested domains over France, with finest horizontal mesh size of 3 km over the Mediterranean area. The initial and coupling fields are derived from the ERA40 reanalysis. Finally, the 10 m wind distributions are reconstructed by weighting each simulation by the corresponding wind class frequency. Evaluation and uncertainty assessment of each step of the procedure is performed. This method is then applied for a climate change impact study: daily 850 hPa wind fields from 14 general circulation models of the CMIP3 multimodel dataset are used to determine evolutions in the frequency of occurrence of the wind classes and to assess the potential evolution of the wind resources in France. Two time periods are focused on: a historical period (1971–2000) from the climate of the twentieth century experiment and a future period (2046–2065) from the Intergovernmental Panel on Climate Change (IPCC) Special Report on Emissions Scenarios (SRES) experiment. Evolution of the 10 m winds in France and associated uncertainties are discussed. Significant changes are depicted, in particular a decrease of the wind speed in the Mediterranean area.

KEY WORDS downscaling; mesoscale modelling; surface winds; climate change; wind energy

Received 15 August 2008; Revised 19 November 2009; Accepted 21 November 2009

1. Introduction

Wind energy is a fast growing renewable energy. Over the past ten years, global wind power capacity has grown at an average annual rate of about 30% (Global Wind Energy Council, 2007). As the life span of modern onshore wind farms is about 20 years, it is of great interest to assess the potential impact of climate change on the wind energy resources over the next decades.

The surface winds are mainly driven by the large scale circulation (LSC). However, several local features such as the surface roughness and the orography modify the spatial and temporal features of the surface winds. Because of their coarse resolution, general circulation models (GCMs), cannot represent the small spatial scale variability of the near surface winds (Pryor and Schoof, 2005). However, they show reasonable skill in simulating the global climate and the LSC. To bridge this scale gap, different downscaling strategies have been developed (Wilby *et al*., 2004). They consist in deriving the local climate state from the GCM's coarse resolution climate state (Giorgi and Mearns, 1991).

In the literature, only a few studies deal with the impact of climate change on wind energy resources. Most of them were performed using statistical downscaling algorithms (Bogardi and Matyasovszky, 1996; Sailor *et al*., 2000; Pryor and Schoof, 2005; Pryor *et al*. 2005b, 2006; Jiménez *et al*., 2008; Najac *et al*., 2009). One advantage of the statistical downscaling approach is that the transfer functions that relate local winds to GCM large-scale variables may be easily applied to several GCMs. This enables a multimodel approach that reinforces confidence in the results and provides an estimation of the uncertainty of the potential changes. Other advantages include the facts that it is computationally inexpensive and can provide specific site information which is very relevant in case of complex orography. Drawbacks include the stationarity hypothesis of the transfer function, the hypothesis that climate change can be viewed as variations in

* Correspondence to: Laurent Terray, Climate Modelling and Global Change Team, CERFACS/CNRS, SUC URA1875, 42 Avenue Gaspard Coriolis, 31057, Toulouse Cedex 1, France. E-mail: terray@cerfacs.fr

the occurrence and intensity of existing synoptic patterns and the lack of relevant observations. Such studies were performed by Pryor *et al.* (2005b) and Pryor *et al.* (2006) for northern Europe using respectively five and ten GCMs, and Najac *et al.* (2009) for France using 14 GCMs. However, a limitation of those approaches relies on their dependance on wind observational data from meteorological stations. For instance, Sailor *et al.* (2000) use three stations over Texas and California, Bogardi and Matyasovszky (1996) seven stations over Nebraska, Pryor and Schoof (2005) and Pryor *et al.* (2005b, 2006) 46 stations over northern Europe, Najac *et al.* (2009) 78 stations over France. Alternatively, Pryor *et al.* (2005a) use a regional climate model (RCM) to dynamically downscale near-surface wind fields. They provide results with high spatial resolution ($0.44 \times 0.44^{\circ}$ horizontal resolution) but use only two GCMs to force their RCM. Indeed such a method requires simulations that are computationally very expensive.

An alternative procedure to statistical- or dynamical-only downscaling was introduced by Frey-Buness *et al.* (1995). Following previous studies (Wippermann and Gross, 1981; Heimann, 1986), their approach is based on the assumption that the climate of a given region may be characterized by the frequency distribution of classified large-scale weather situations. They first define 48 large-scale weather types according to some synoptic similarities. Then a simulation is performed for each large-scale weather type with a hydrostatic mesoscale model whose horizontal resolution varies between 20 and 30 km. The individual simulation results are then weighted by the frequency of the corresponding weather types. Eventually they obtain fine mesh wind distributions. This procedure is applied to the Alpine region for a global climate simulation of the present January climate. Mengelkamp *et al.* (1997) and Mengelkamp (1999) applied the same procedure to estimate wind climatologies over an area of central Germany for the present climate.

In this paper we follow the main ideas of the methodology described by Frey-Buness *et al.* (1995) and apply a similar approach for France. We use a non-hydrostatic mesoscale model with three nested domains with the middle one covering the whole of France at a 9-km horizontal resolution. The inner one covers the southeast of France at 3-km resolution. We apply this method to estimate the impact of climate change on the near-surface winds in France with a multimodel approach. The main advantage of this hybrid method is to combine a multimodel approach in terms of the large-scale predictors with a complete and high spatial resolution for the predictands which are provided by the mesoscale model.

In Section 2, the data and model used for the study are presented. The different steps of the method and their validation are described in Section 3. In Section 4, we apply the downscaling algorithm with several GCMs for a historical period (1971–2000) and a future period (2046–2065). Conclusions and perspectives are presented in Section 5.

2. Data and Model Description

2.1. Near-surface wind speed observations

Daily mean 10-m wind speeds and directions were extracted from the Météo-France (French meteorology service) SQR (Série Quotidienne de Référence) dataset (Moisselin *et al.*, 2002). Daily wind speeds have been obtained by averaging 24 hourly values of wind speed measurements. Daily wind direction is taken as the direction of the maximum hourly value of the wind speed measurements. The dataset does not include hourly wind components and it is thus not possible to calculate the daily average wind direction which is potentially the optimal approach for our study. We use wind speed and direction from this dataset at 78 stations over France for the period 1974–2002 (Figure 1). The quality control of this dataset has been carried out by the Division de la Climatologie (DCLIM) service of Météo-France. In France, two main regions exhibit a strong potential for wind resources: the northwest and the southeast. The sorthwest benefits from south-westerly and westerly winds that blow from the Atlantic Ocean. In the southeast, the complex topography constrains and accelerates the large-scale meridional wind flow due to the location of the mountain ranges. In particular, two natural channels, the Rhone valley between the Alps and the Massif Central and the valley between the Pyrenees and the Massif Central (Figure 1), generate strong northerly and north-westerly winds called respectively Mistral and Tramontana. Due to the complex orography, surface winds over France display a large spatial variability at small spatial scale which cannot be accurately represented in global climate models. Dynamical and/or statistical downscaling is thus necessary to study the changes of the surface winds due to anthropogenic forcing.

2.2. ERA40 reanalysis

Zonal and meridian components of the daily mean 850 hPa wind over the period 1974–2002 were derived from the European Centre for Medium-Range Weather Forecasts (ECMWF) ERA40 reanalysis (Uppala *et al.*, 2005). 0000 UTC, 0600 UTC, 1200 UTC and 1800 UTC values at a $2.5^{\circ} \times 2.5^{\circ}$ resolution were daily averaged. The predictor domain is represented in Figure 1.

2.3. CMIP3 multimodel dataset

For the future climate study, we use daily mean 850 hPa wind fields from 14 coupled atmosphere–ocean general circulation models (AOGCM) of the World Climate Research Programme's (WCRP's) Coupled Model Intercomparison Project phase 3 (CMIP3) multimodel dataset, according to the daily data availability: BCCR-BCM2.0, CGCM3.1(T63), CNRM-CM3, CSIRO-Mk3.0, GFDL-CM2.0, GFDL-CM2.1, GISS-AOM, FGOALS-g1.0, INM-CM3.0, IPSL-CM4, MIROC3.2(medres), ECHO-G, ECHAM5/MPI-OM, MRI-CGCM2.3.2. Detailed documentation of the CMIP3 models can be found at http://www-pcmdi.llnl.gov/ipcc/model_documentation/

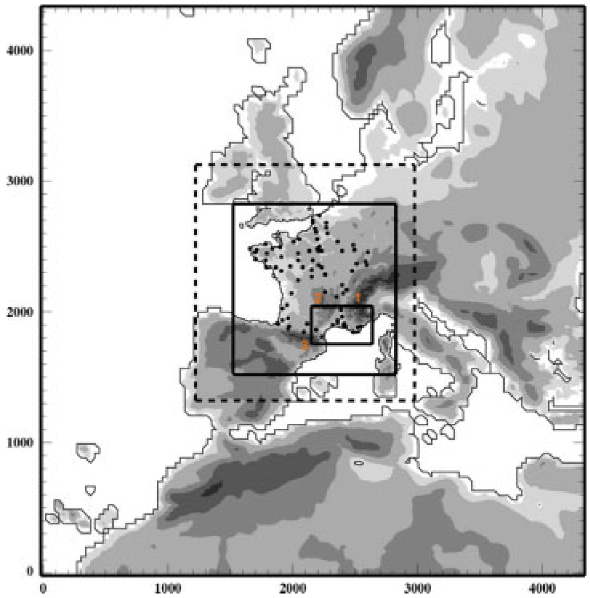

Figure 1. The three Meso–NH domains are indicated by the black solid squares, the predictor domain by the black dashed square and the 78 SQR dataset stations by the dots. Six orographic levels are represented: 0, 100, 500, 1000, 2000, 3000 meters. Numbers 1, 2 and 3 indicate the three major French massifs: the Alps, the Massif Central and the Pyrenees. This figure is available in colour online at wileyonlinelibrary.com/journal/joc

ipcc_model_documentation.php. The horizontal resolution of these models varies between $1.875° \times 1.875°$ and $4° \times 5°$. Daily mean 850 hPa wind fields have been interpolated onto the ERA40 $2.5° \times 2.5°$ grid. Two time periods are focused on: a historical period (1971–2000) from the climate of the 20th century experiment with the observed anthropogenic forcing and a climate projection period (2046–2065) from the IPCC SRES A1B experiment and scenario.

2.4. Méso–NH model

Méso–NH is a non-hydrostatic mesoscale model that has been jointly developed by the CNRM (Centre National de la Recherche Météorologique) and by the Laboratoire d'Aérologie (Lafore *et al*., 1998). This multidimensional model integrates an anelastic system of equations and allows for simulations of atmospheric flow ranging from the meso-alpha scale down to the microscale. The three components of the wind and the turbulent kinetic energy are prognostic variables. Simulations at different scales can be done with the two-way interactive grid nesting technique (Stein *et al*., 2000). More details about Méso–NH can be found on the website (http://www.aero.obs-mip.fr/mesonh/).

The simulations were performed with Méso–NH over three nested domains: the first domain covers a 4300×4300 km^2 area centred over western Europe with a 36-km horizontal resolution, the second domain a 1300×1300 km^2 area centred over France with a 9-km horizontal resolution, the third domain a 480×290 km^2 area centred over south-eastern France with a 3-km horizontal resolution (Figure 1). There are 40 vertical levels from 0 m to 20 km, the vertical resolution varying between 20 m near the ground to 1200 m for the highest levels. All model domains use two-way grid-nesting interactions. Simulations are performed for 24 h after a 6-h spin-up. Boundary and initial conditions of the largest domain are provided by the ERA40 reanalyses, updated every 6 h.

3. Method

3.1. Introduction

As introduced by Frey-Buness *et al*. (1995), our approach relies on the assumption that the local climate may be characterized by the frequency of occurrence of classified large-scale weather types. Under future climate conditions, the frequency of occurrence of those weather types might be modified, but their dynamical characteristics are assumed to remain unchanged. The relevance of this approach is supported by some studies which suggested that anthropogenic climate change may manifest itself as a projection onto the pre-existing natural modes of variability of the climate system (Corti *et al*., 1999; Stone *et al*., 2001).

The construction of our downscaling algorithm consists of the choice of the predictors and two steps summarized in Figure 2:

(1) Choice of predictor: the 850 hPa wind field (UV850) is a large-scale variable that exhibits strong dynamical links with the 10 m winds. Accordingly, it has been shown to be a relevant predictor for 10 m wind downscaling in several previous studies (Frey-Buness *et al*., 1995; Sailor *et al*., 2000; Najac *et al*., 2009).
(2) Step 1: daily UV850 from the ERA40 reanalysis is thus used to define weather types over the period 1974–2002 as in Najac *et al*. (2009). The weather types are then subdivided into a large number of wind classes and one day is randomly selected inside each wind class.
(3) Step 2: mesoscale simulations of each selected day are performed with Méso–NH.

Then, the UV850 simulated by a GCM over any period of time is used to compute the frequency of occurrence of the wind classes over this period. Finally, each mesoscale simulation is weighted by the frequency of occurrence of the corresponding wind class so that 10 m wind speed and direction distributions are provided at the horizontal resolution of the different Méso–NH domains. We discuss the algorithm in more details in the following sections after the description of a validation diagnostic based on wind roses.

3.2. Validation diagnostic: wind roses

In the following sections, 10 m wind roses are only used to validate different steps of the method. We adopt here the wind rose categories as used operationally by Météo France forecasters:

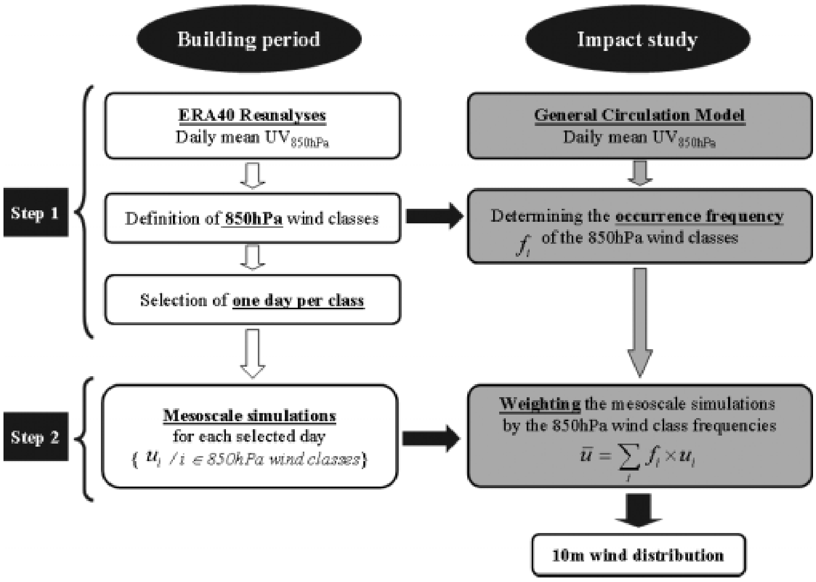

Figure 2. Flow chart of the downscaling procedure.

- One category for low wind speeds (U10 < 1.5 m/s) which encompasses all wind directions
- three other wind speed categories, which are subdivided into 18 wind direction categories (every 20°)

1.5 m/s $\leq$ U10 $<$ 4.5 m/s
4.5 m/s $\leq$ U10 $<$ 8.5 m/s
8.5 m/s $\leq$ U10.

The wind roses are thus composed of 55 categories ($1 + 18 \times 3$). A quality criterion C has been defined in order to measure the similarity between the reconstructed and the observed wind roses:

$$C = 100 - \frac{1}{2}\sum_{i=1}^{55} |f_i^{\text{obs}} - f_i^{\text{rec}}|$$

where f_i^{obs} is the absolute frequency of the category i of the observed wind rose, and f_i^{rec} the absolute frequency of the category i of the reconstructed wind rose. Therefore, C is equal to 0 when the wind roses are totally disjointed and equal to 100 when they perfectly match. These non-normalized wind rose quality criteria are a useful tool that enables to account for biases in both wind speed and direction.

3.3. Step 1: day selection

3.3.1. Method

The first step consists in defining wind classes. We start from the weather type classification performed by Najac *et al.* (2009). Considering two seasons (an extended winter season from October to March called ONDJFM and an extended summer season from April to September called AMJJAS), they perform a weather type classification of the UV850 of the ERA40 reanalysis, over the period 1974–2002, in the subspace spanned by the leading UV850 empirical orthogonal functions (EOFs). The classification is performed with the k-means algorithm. They find six weather types for both ONDJFM and AMJJAS (Figures 3 and 4). They show that those weather types represent classical synoptic situations over France. They also assess the relevance of the weather type classification with regard to 10 m wind properties (for instance, minimization of the 10 m wind speed and direction intra-type variance). In the following sections, the statement ‘weather types’ will refer to the weather types described in Najac *et al.* (2009).

Similar weather type approaches have been shown to be a useful tool to identify dominant modes of circulation variability (Conil and Hall, 2006) and to analyse the links between the LSC and the local climate (Plaut and Simonnet, 2001; Cassou *et al.*, 2005). However, under a given climate perturbation, expected modifications of the local climate may occur in two different ways (Boé *et al.*, 2006): changes in the weather type occurrences (inter-type modifications) and changes in the distribution of the days within the weather types (intra-type modifications). Intra-type variability can be defined as the residual variability of the local climate within a given weather type. It relies upon the simple argument stating that the local climate (here the surface winds) cannot be fully determined from the LSC (here the UV850). Changes in intra-type variability may be as (or even more) important than inter-type modifications. It is thus necessary to take them into account in the downscaling approach. As a result, each of the weather types has been subdivided into a number of smaller wind classes in order to deal with the surface wind variability within the weather types and to account for intra-type changes. For each weather type, we have computed the Euclidean distances between each daily 850 hPa wind pattern (belonging to the given weather type) and all the weather type centroids in the space spanned by the leading UV850 EOFs as defined in Najac *et al.* (2009). Then, for each weather type, we have determined the distance that has the

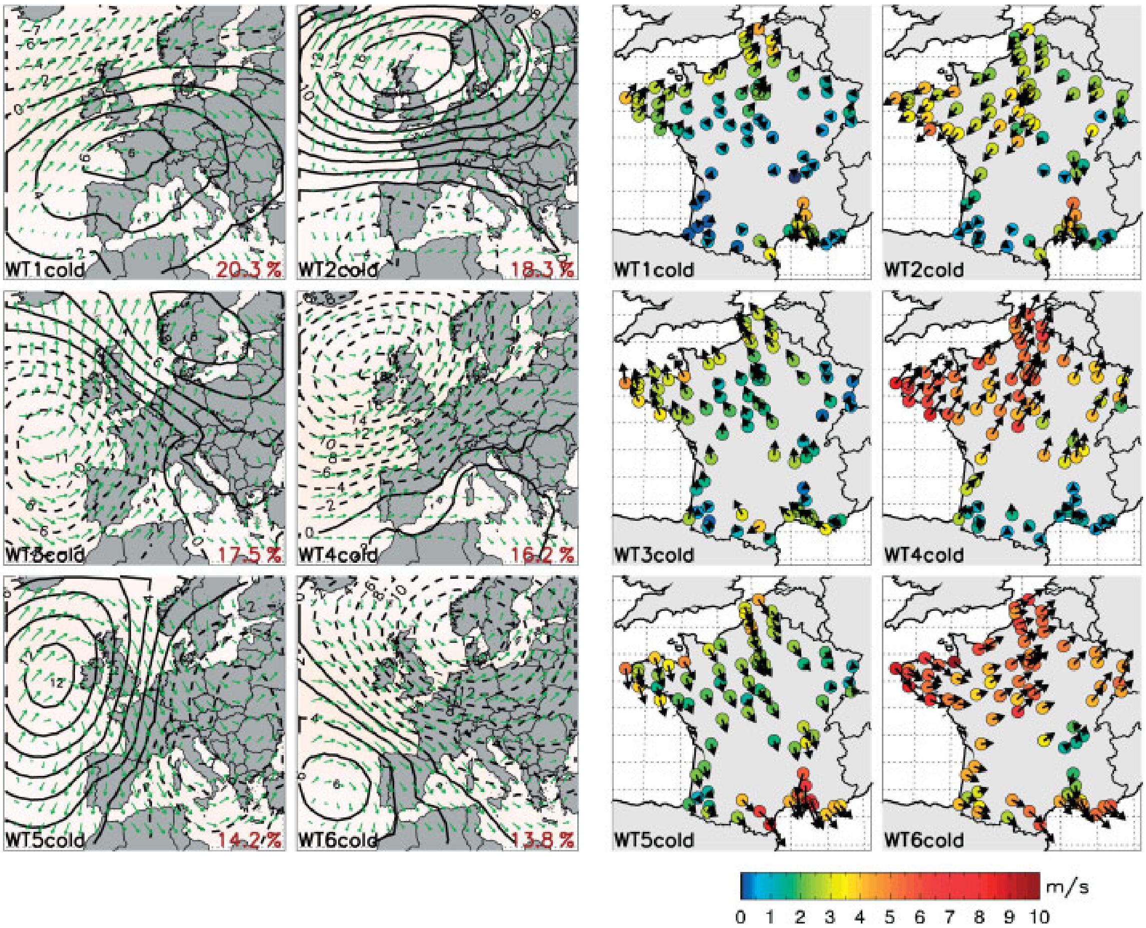

Figure 3. SLP anomaly (contours every 2 hPa) and 850hPa wind (arrows) composites (left panel), and 10m wind composites (m/s) (right panel) for the weather types of ONDJFM (cold season) (1974–2002). Similar to Figure 3 from Najac *et al*. 2009. Left panel: arrows indicate wind directions, arrow length represents the magnitude of the wind vector (varying between 0 and 18 m/s). Right panel: color shading represents wind magnitude and arrows indicate wind directions (note that arrow length is also proportional to wind magnitude). Weather type occurrence (%) is indicated in the bottom right-hand corner of each panel.

largest linear correlation with the 10 m wind components. For example, for the weather type WT2cold, we found that the distances to the centroid of the weather type WT4cold provided the largest linear correlations with the 10 m wind components. Then, each weather type has been subdivided into quantiles of the retained distance. The number of quantiles depends on the frequency of occurrence of the weather types: this means that the higher the frequency of occurrence of a given weather type, the greater the number of wind classes within this weather type and thus the greater the number of quantiles. For instance, the weather type WT2cold whose frequency of occurrence is about 18.3% has 18 quantiles or wind classes. Finally, one day has been randomly selected within each wind class. We thus get a sample of days for each season which is expected to be suitable to estimate the 10 m wind speed and direction distributions (see Najac, 2008 for a thorough description and illustration of these points).

3.3.2. *Size of the day samples*

The total number of wind classes defines the size of the sample of selected days. As the mesoscale simulations are very time consuming, only a small number of days can be selected. According to the available computing resources, about 300 simulations was a maximum. In order to define the size of the samples, we have computed the wind rose quality criteria at each station, for each season and for different sample sizes (from 10 to 200) over the period 1974–2002. Here, observed wind roses are computed using the observed wind speeds and directions from the whole SQR dataset, and reconstructed wind roses by weighting the observed wind speed and direction of the selected days by the corresponding 850 hPa wind class frequencies. As days are selected at random, for each sample size we have repeated the procedure 1000 times in order to get an estimation of the robustness of the resulting quality criteria.

The evolution of the mean quality criterion (averaged over all stations) as a function of the sample size is shown in Figure 5. As expected, the quality criterion increases with the sample size while the dispersion decreases: the larger the size of the sample of selected days, the better the estimation of the 10 m wind properties. It can also be seen that the behaviour of the curve becomes asymptotic. This

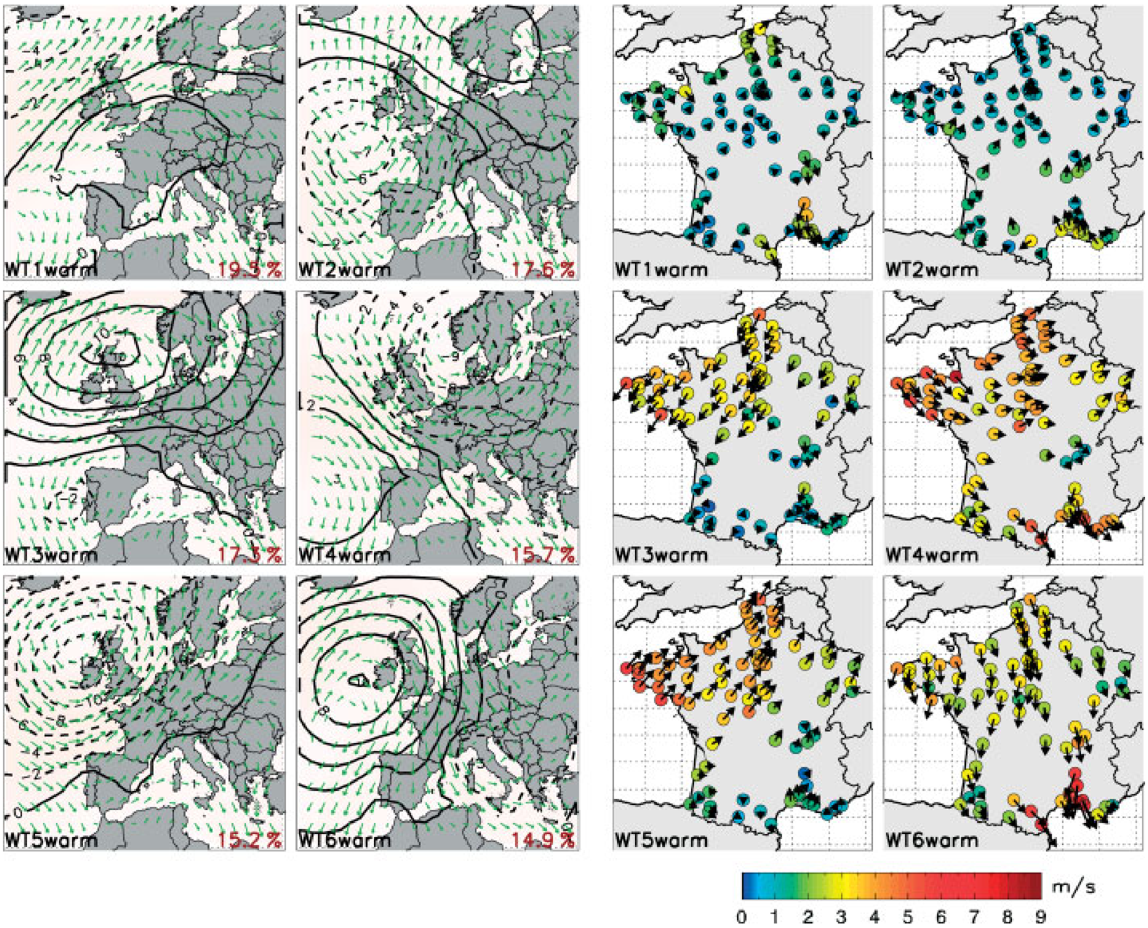

Figure 4. Same as Figure 4, but for AMJJAS (warm season). Similar to Figure 4 from Najac *et al*. 2009.

means that, from a certain size, increasing the sample size will not significantly improve the quality criteria whereas it will largely increase the computing time.

As we will see in Section 3.2.4, the quality criterion is not homogeneous over France: some areas exhibit high quality criteria, while other areas exhibit lower quality criteria. For a given classification, the difference between the highest and the lowest quality criteria is thus another indicator of the relevance of this classification. Figure 5 shows the evolution of this difference, averaged over the 1000 classifications, as a function of the sample size. It can be seen that this difference and the dispersion of this difference decrease with the sample size. However, the behaviour of the curves becomes also asymptotic. While there is a significant improvement when increasing the sample size for small sample sizes, the improvement for large sample sizes is poor considering the computing time cost.

Finally, we estimated that 100 days for ONDJFM and 100 days for AMJJAS were a good compromise (quality criterion close to 80 and about 6 months of computing time with Meso–NH for 200 simulations).

3.3.3. Comparison with other partitioning methods

Other variants of the main method have been tested in order to assess the performance of our choice, from the simplest method that consists in randomly choosing 200 days among the whole 1974–2002 period to more complex methods involving different classification algorithms. The quality criteria averaged over all stations for each season and different methods are presented in Table I. When a random process is involved in the method, the procedure is repeated 1000 times in order to provide an estimation of the robustness of the results. It can be seen that all methods provide close results. However, for both seasons, our method provides the best results among the methods that use a random process. The best partition calculated with our method provides also the best results among the deterministic methods ($78.3 + 0.4$ is the highest value in ONDJFM and $79.6 + 0.4$ in AMJJAS). Furthermore, our method presents three advantages in a climate change perspective:

(1) it is based on robust weather types that have been shown to allow useful physical interpretations of climate change impacts on surface winds (Najac *et al*., 2009);
(2) the intra-type variability is handled by means of the wind classes that have been defined within the weather types;
(3) for a given criterion, deterministic methods enable to define the best partition for the present climate. However, this may change under perturbed climate

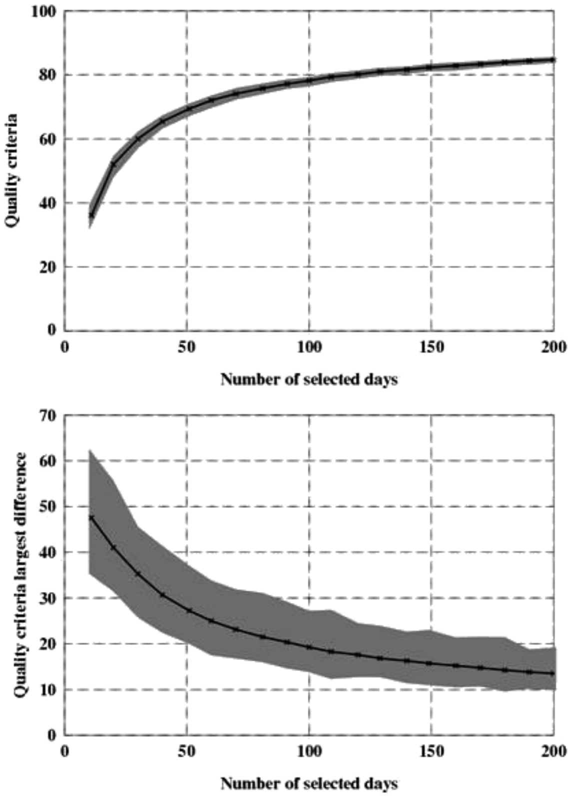

Figure 5. Upper panels: evolution of the mean wind rose quality criteria (averaged over all stations and the 1000 classifications) as a function of the number of selected days, for ONDJFM (left panel) and AMJJAS (right panel). The grey curves indicate the range between the minimum and maximum values of the quality criteria over the 1000 classifications. Lower panels: wind rose quality criteria have been computed at each station for each classification. For each classification, the difference between the highest and the lowest quality criteria is calculated. The black curve indicates the evolution of this difference averaged over the 1000 classifications as a function of the number of selected days. The grey curves indicate the range between the minimum and maximum values of this difference over the 1000 classifications.

Table I. Mean wind rose quality criteria (averaged over all stations) obtained with 6 different methods of day selection.

	1	2	3	4	5	6
ONDJFM	77.8 (±0.6)	78.1 (±0.5)	78.4	77.7 (±0.4)	78.4	78.3 (±0.4)
AMJJAS	79.2 (±0.6)	79.5 (±0.4)	78.8	78.9 (±0.4)	79.9	79.6 (±0.4)

(1) days randomly chosen/(2) days randomly chosen within the weather types/(3) direct classification of the UV850 into 100 wind classes and days chosen near the wind classes centroids/(4) direct classification of the UV850 into 100 classes and days randomly chosen within the wind classes/(5) reclassification of the weather types into wind classes and days chosen near the wind class centroids/(6) reclassification of the weather types into wind class and days randomly chosen within the wind classes. When a method involves a random process, 1000 classifications are performed and the amplitude between the lowest and the highest value of the mean quality criteria is indicated between brackets. All the classifications in these different methods have been performed with the k-means algorithm.

as the best partition for the present climate will not necessarily be the best partition for the future climate. Accordingly, the random process used in our method implies that all days that belong to a given wind class may constitute a good representative sample of this wind class for different climate conditions. Thus, such a procedure prevents from favouring the performance of the downscaling method over the historical period compared with the future periods.

3.3.4. *Final validation of the step 1*

Finally, Figure 6 shows the value of the quality criteria at each station for both seasons. Here, observed wind roses are computed using the observed wind speeds and directions from the whole SQR dataset, and reconstructed wind roses by weighting the observed wind speed and direction of the selected days by the corresponding 850 hPa wind class frequencies. Results are satisfactory with quality criteria higher than 70 at all stations and for both seasons. Results are globally similar for both seasons (the mean quality criterion is equal to 79 for both the ONDJFM and AMJJAS seasons). It can be noticed that the quality criteria are lower in the northwest and along the coasts. This is due to the fact that the 10 m wind speed and direction temporal variability are higher in those regions. On the contrary, in the channels

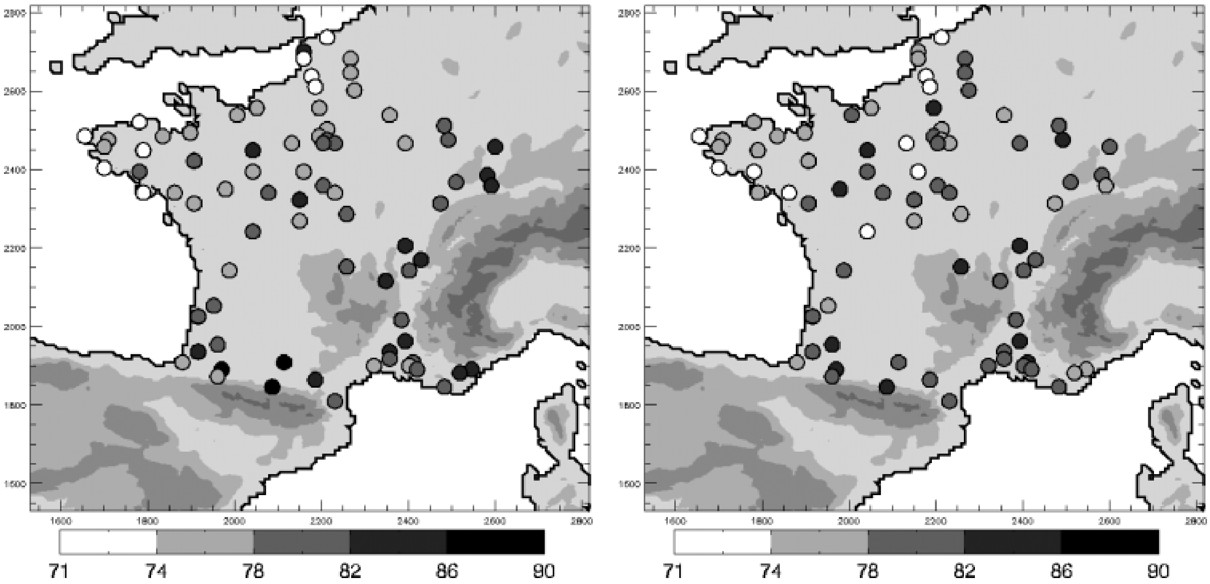

Figure 6. Quality criteria in ONDJFM (left panel) and AMJJAS (right panel) using observations for the selected days (1974–2002). Four orographic levels are represented: 0, 500, 1000, 2000 meters.

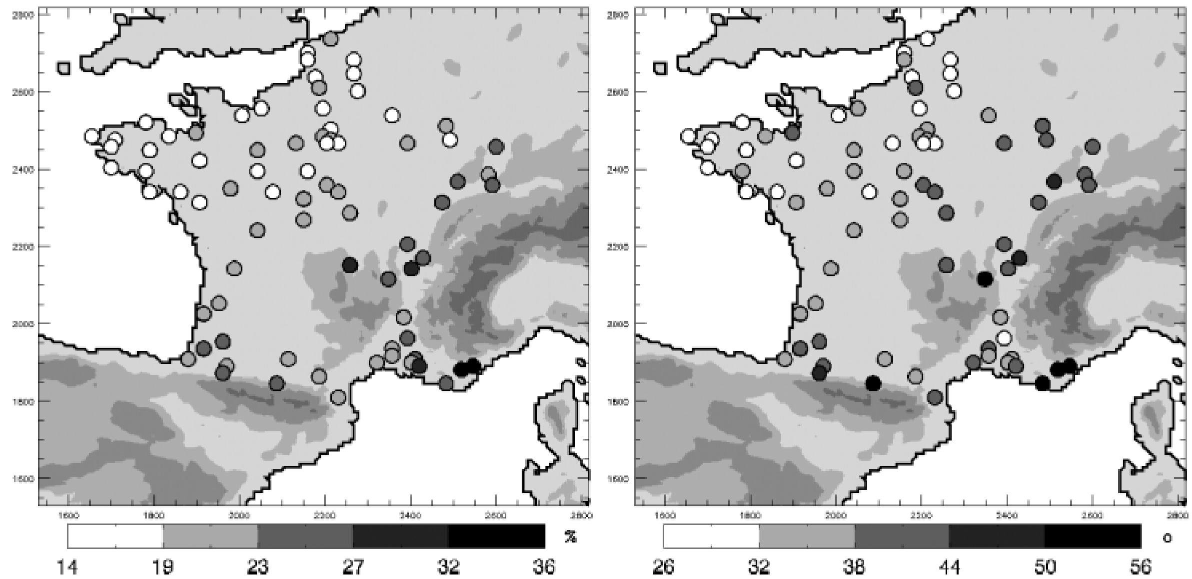

Figure 7. For the 9-km domain, mean absolute errors between observed and simulated daily mean 10m wind speeds (left panel) (in percent) and directions (right panel) for the 200 simulated days (100 for ONDJFM and 100 for AMJJAS). The orographic levels are the same as in Figure 7.

between the Pyrenees and the Massif Central (south of France), and between the Massif Central and the Alps (southeast of France), the wind flow is constrained by the orography into a few dominant directions. As a result, the temporal variability of the 10 m wind direction is lower, and the quality criteria are generally higher.

3.4. Step 2: mesoscale simulations

Mesoscale simulations with the Méso–NH model (see Section 2.4) have been performed for each one of the 200 selected days. For each station and each day, the daily mean 10 m wind speed and direction simulated by Méso–NH at the nearest grid-point were compared with the SQR observed values. Figure 7 shows the results for the 9-km domain. The highest discrepancies for both the wind speed and direction are found near mountains in the south, the southeast and the East. Indeed, in those regions, the wind flow is constrained by a complex orography. While at large scale, this should lead to a high spatial consistency of the wind speed and direction, small-scale orographic effects can perturb the large-scale homogeneity and induce high small-scale spatial variability. As a result, the wind conditions observed at the stations may be significantly different from the wind conditions simulated at the nearest-grid point. Accordingly, discrepancies for both the wind speed and direction decrease when getting away from mountains (the lowest discrepancies are thus found in the northwest).

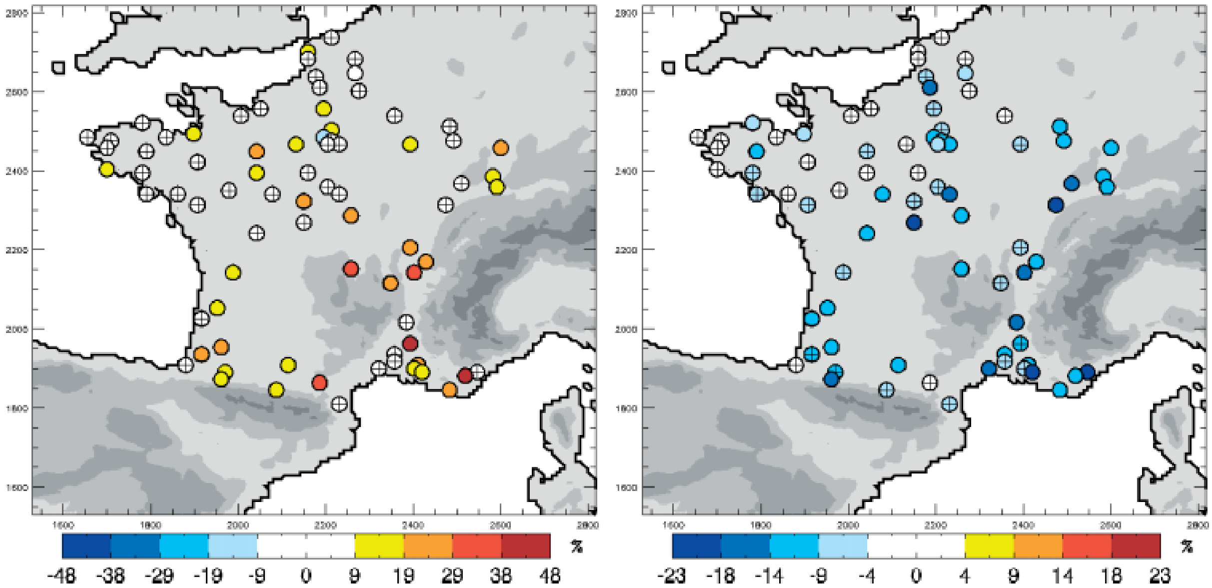

Figure 8. For the 9-km domain, mean errors (in percent) between observed and simulated daily mean 10m wind speeds for the low wind days (left panel) and the high wind days (right panel). Low (high) wind days are defined at each station as the days for which the observed wind speed is lower (higher) than the median. We thus get 100 high wind days and 100 low wind days for each station. Stations where errors are not statistically significant are indicated by crosses (T-test, 0.05 level).The orographic levels are the same as in Figure 7.

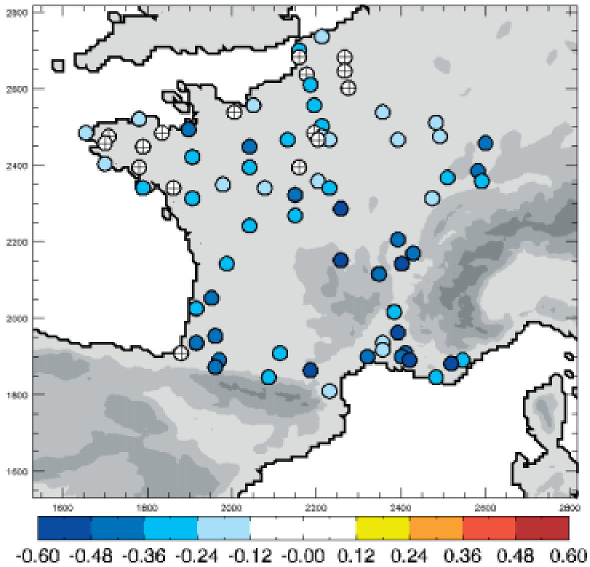

Figure 9. Linear correlation coefficients between the observed wind speeds and the relative differences between observed and simulated wind speeds. Stations where the correlation is not statistically significant are indicated by crosses (0.05 level). The orographic levels are the same as in Figure 7.

Furthermore, we found that the Meso–NH model generally underestimates high wind speeds and overestimates low wind speeds. This is shown in Figure 8, where the mean errors have been computed at each station for the high wind days and the low wind days separately. It can be seen that these biases are found in almost all stations. Then, Figure 9 shows the linear correlation coefficients at each station between the observed wind speeds and the relative differences between simulated and observed wind speeds. Many stations exhibit high correlation coefficients (in absolute value). This confirms our previous remark: for low observed wind speeds, differences are large and positive (overestimation); when the observed wind speeds increase, differences decrease until being negative; when observed wind speeds get stronger, then differences get large and negative (underestimation).

In the southeast, results are not significantly improved with the 3-km domain, neither for the wind speed nor for the wind direction (not shown). This may suggest that the additional value of using the 3-km domain, which is very computing time demanding, is limited. However, as the simulations have been performed with two-way grid-nesting interactions, results from the 9 km may benefit from the better representation of the dynamical and physical processes with the 3-km domain. Confirming this hypothesis would require to perform new simulations without the 3-km domain and to compare the results. Actually, it is likely that the 3-km resolution still remains too low to deal with the very complex orography of the south-east of France, especially in the eastern part of the area (south of the Alps).

3.5. Validation of the whole procedure

Final wind roses are reconstructed by weighting the mesoscale simulations by the corresponding wind class frequencies and compared to the observed wind roses. These roses then account for both sources of error, the day sampling and the numerical simulations performed with the mesoscale model. As shown by Figure 10, the quality criteria are lower than on Figure 6. Averaged over all stations and both seasons, the quality criterion has decreased from 79 to 70. While the lowest quality criteria on Figure 6 were found in the northwest and along the coasts, they are now situated in the southeast. Differences between Figure 10 and Figure 6 can be explained by the

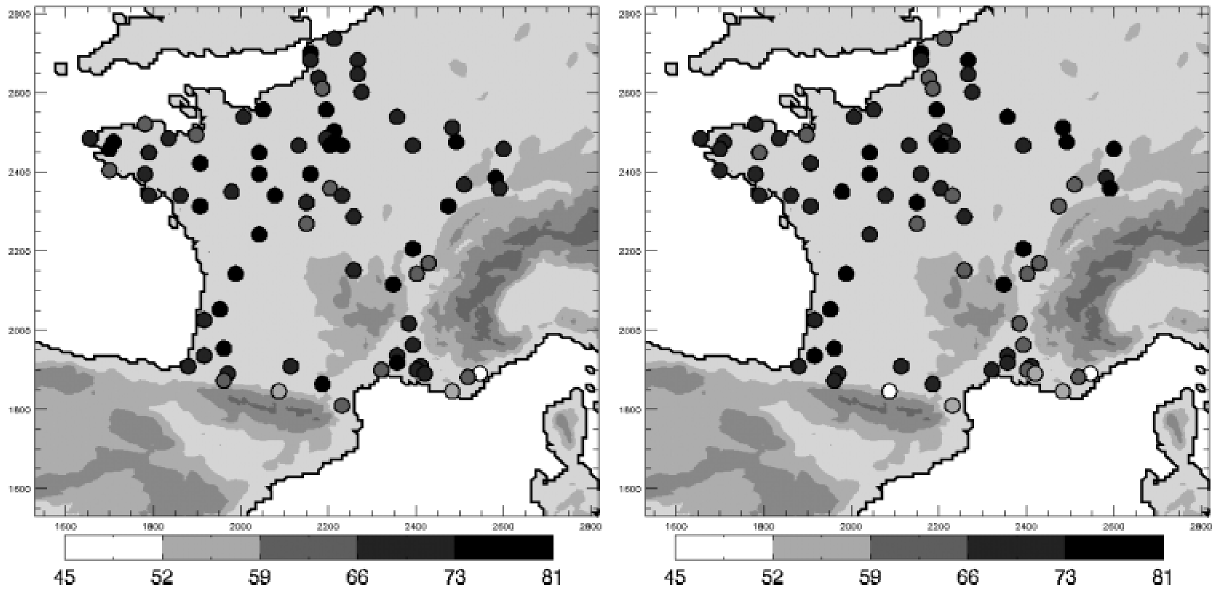

Figure 10. Quality criteria in ONDJFM (left panel) and AMJJAS (right panel), using the Méso-NH simulations for the selected days (1974–2002). The orographic levels are the same as in Figure 7.

fact that errors originating from the day sampling (Section 3.2) and errors originating from the numerical simulations (Section 3.3) add up. At each station, we can evaluate the relative weight of each one of these two parts. This is shown on Figure 11. As expected, errors that originate from the numerical simulations predominate in stations situated in the mountainous areas of the south and southeast of France, while, in the northwest of France, the main fraction of the errors is due to the day sampling. This is coherent with what we found in Sections 3.2.4 and 3.3. Finally, errors that originate from the day sampling predominate in most stations (69 stations over 78).

4. Impact study

4.1. Methodology

We use the daily 850 hPa wind fields from the 20th century simulations with observed anthropogenic forcings performed with 14 CMIP3 models as predictors (see Section 2.3). For each CMIP3 model, the UV850 anomalies are computed using the historical period climatology. Then, the UV850 anomalies are projected onto the learning period ERA40 UV850 EOFs, and the frequency of occurrence of the wind classes is computed for each model, each period and each season. Finally, for each model, each period and each season, the Méso–NH simulations are weighted by the corresponding wind class frequencies.

4.2. Historical period

4.2.1. Predictor validation

First of all, the ability of the models to properly reproduce the UV850 mean states within the weather types over the historical period is assessed by means of Taylor diagrams

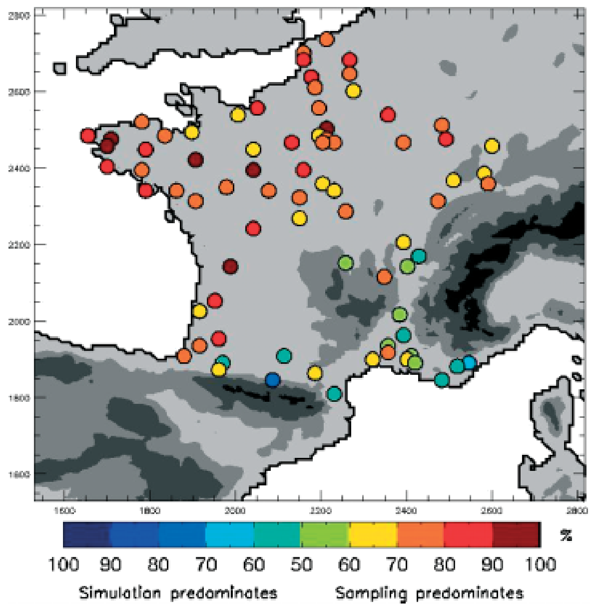

Figure 11. Percentage of the wind rose errors explained by the day sampling and the numerical simulations respectively. Stations where errors that originate from the day sampling (numerical simulation) predominate are red (blue). The orographic levels are the same as in Figure 7.

(Taylor, 2001) (Figure 12). Those diagrams provide a concise statistical summary of how well spatial patterns match each other in terms of their pattern correlation, their root-mean-square difference and the ratio of their spatial variances. Here we compare the weather types as simulated by the CMIP3 models forced by the observed anthropogenic forcing over the 1971–2000 period with those present in ERA40 over the same period. First of all, it can be seen that the pattern correlations are generally high (higher than 0.6 in most cases). Second one can notice that the variance is generally underestimated by

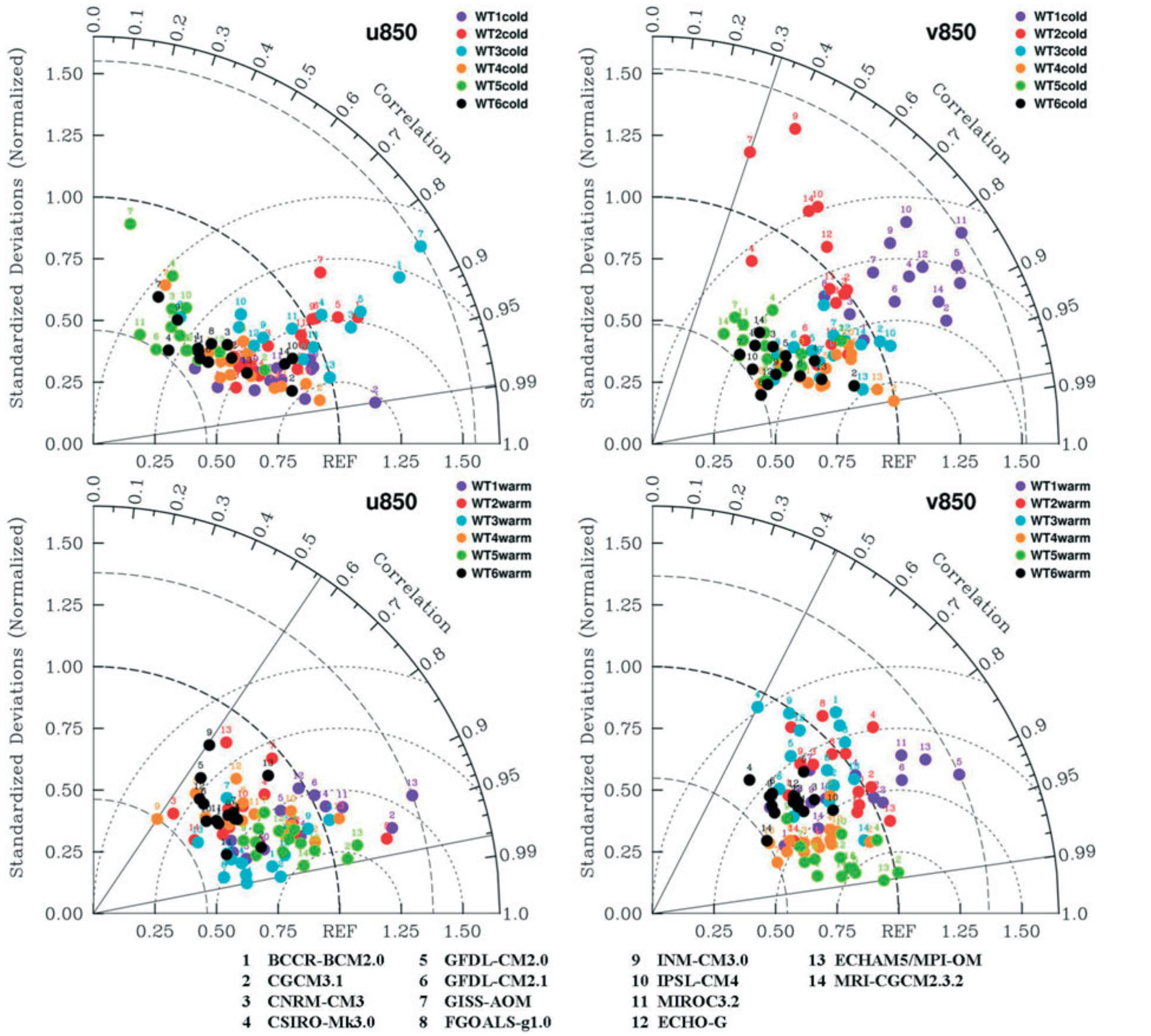

Figure 12. Taylor diagram for the mean zonal (left panel) and meridional (rignt panels) 850hPa wind components of each weather type in ONDJFM (upper panels) and AMJJAS (lower panels) of the historical period (1971–2000). The horizontal and vertical axes represent the ratio of the spatial standard deviations of the reference (ERA40) and simulated (CMIP3) fields. The radial axis indicates the spatial correlation between the reference and simulated fields. The distance between the origin (noted REF) and any point is proportional to the root-mean-square difference.

the models, whatever the weather type or the season. This was actually expected. Indeed most models have a horizontal resolution lower than the ERA40 resolution, therefore the spatial variability of the interpolated fields is likely to be smaller for most models. It is also interesting to note that there is high coherence between the models: they share similar qualities or deficiencies (see the clusters of coloured points).

Then, we compare the frequency of occurrence of the weather types when classifying the UV850 from ERA40 and the CMIP3 models for the historical period (Figure 13). Classification is performed in the subspace spanned by the leading learning period ERA40 UV850 EOFs using the centroids of the learning period weather types. Results with the CMIP3 models are generally close to the reanalysis, except for the weather types associated with a high pressure system centred over France ($WT1_{cold}$ and $WT1_{warm}$) or over the north of the British Isles ($WT2_{cold}$ and $WT3_{warm}$): while the $WT1_{cold}$ and $WT1_{warm}$ occurrences are overestimated and show high dispersion among models (not shown), the $WT2_{cold}$ and $WT3_{warm}$ occurrences are underestimated.

4.2.2. *Downscaling validation*

We first applied the downscaling algorithm for the historical period. Multimodel wind roses are computed by merging all CMIP3 model downscaling results, and the quality criteria are calculated for the 1974–2000 period using the observed wind roses as references. Those quality criteria are then compared to the ones obtained with the ERA40 downscaling (Figure 14 for the 9-km domain). In most cases, the CMIP3 quality criteria are lower but differences are small (the largest difference between the quality criteria is equal to 4). When focusing on the spread of the CMIP3 model downscaling results, no regional structure appears: the agreement between

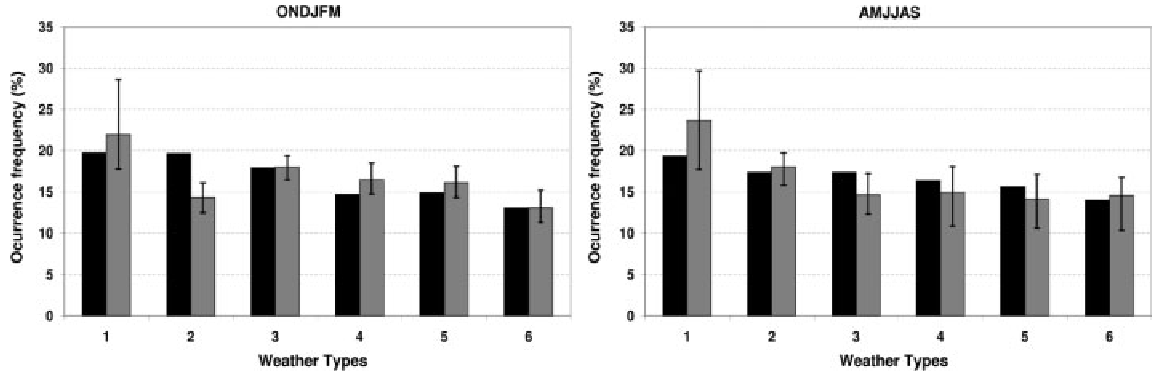

Figure 13. Weather type occurrences in percent for each season when classifying the 850hPa wind fields from ERA40 (black) and the CMIP3 models (dark–grey) (occurrences averaged over all the CMIP3 models) for the historical period 1971–2000. Vertical bars represent the range between the maximum and the minimum values obtained with all models.

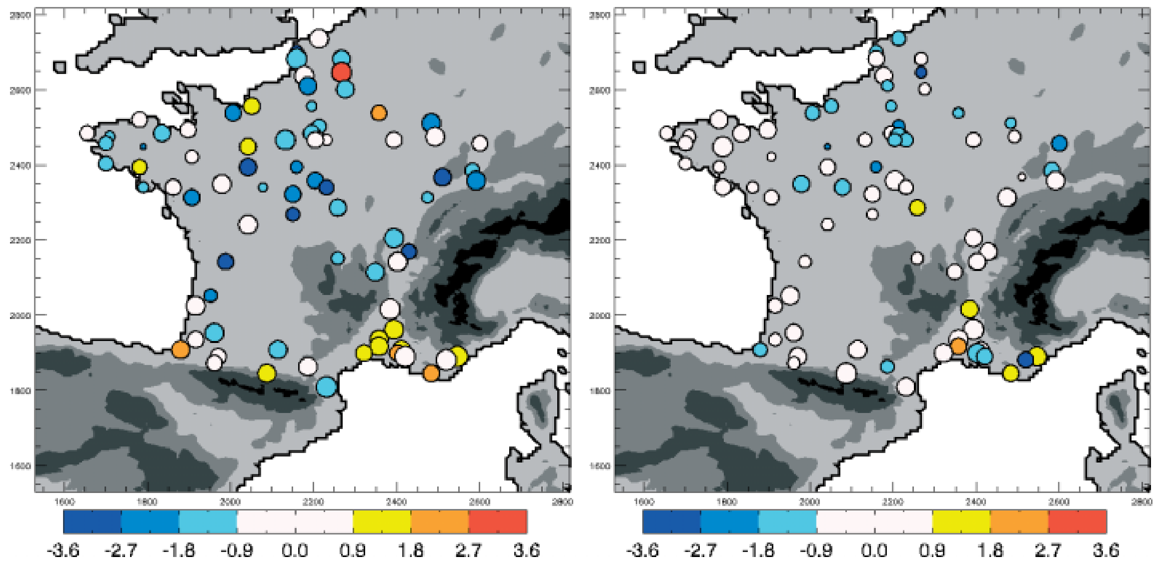

Figure 14. Differences between the wind rose quality criteria computed with the CMIP3 models downscaling and with the ERA40 downscaling, for the period 1974–2000 and the 9-km Méso-NH domain, in ONDJFM (left panel) and AMJJAS (right panel). Circles are inversely related to the multimodel spread (wind roses have been computed for each CMIP3 model separately and the difference between the highest and the smallest quality criteria is calculated at each station): the smallest circle indicates a spread of 16.7 and the largest a spread of 1.5. The orographic levels are the same as in Figure 7.

models is homogeneous over the whole studied domain. On average, the spread is equal to 5 in ONDJFM and 7 in AMJJAS. The larger spread in AMJJAS can be linked to the larger dispersion in the weather type occurrences for this season (Figure 13).

Finally, the averaged quality criterion is equal to 69 in ONDJFM and 69 in AMJJAS with CMIP3 models, while it is equal to 70 in ONDJFM and 69 in AMJJAS with ERA40.

4.3. Climate scenario

4.3.1. Downscaled winds

We now focus on mean changes in the downscaled 10 m winds for the 2046–2065 period relative to the 1971–2000-historical period (Figure 15 for ONDJFM and Figure 16 for AMJJAS). The mean changes are simply estimated as the difference between the climatology of the two periods.

In ONDJFM, the northwest experiences a low increase (maximum of 2.6%) while the Mediterranean area experiences a stronger decrease of the mean 10 m wind speed (maximum of 5.8%). This is associated with a decrease of the westerly, north-westerly and northerly winds over the southeast (decrease of the Mistral and Tramontana events), and an increase of the south-westerly winds over the northwest. Decrease of the wind speeds in the southeast is particularly pronounced in areas where the Mistral and Tramontana winds are usually the strongest: the Rhone valley between the Alps and the Massif Central with an extension over the sea, and the most southern part of France where the Pyrenees reach the Mediterranean sea and which extends far away over the sea. In the northwest, changes are more uniform. Differences between the 9- and 3-km domains are weak, except that results from the 3-km domain obviously provide more details. Most models are in agreement concerning the sign of the changes in those areas (80% of the models agree)

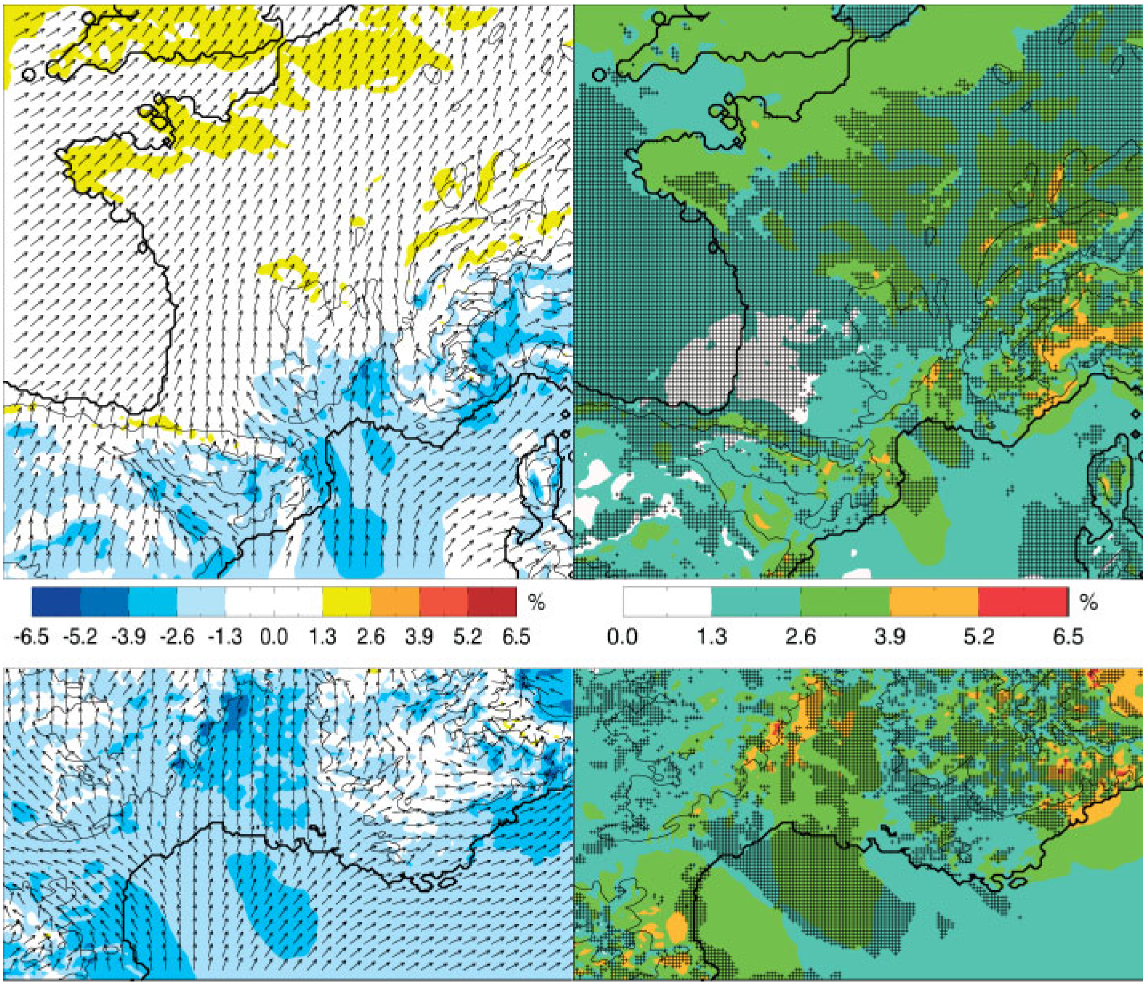

Figure 15. Left panels: multi-model mean 10m wind speed changes in percent and associated vector anomalies for 2046–2065 relative to 1971–2000 in ONDJFM with the 9-km domain (upper-left panel) and the 3-km domain (lower-left panel). Right panels: dispersion among the CMIP3 models (standard deviation formulated as a percentage of the historical period multi-model mean 10m wind speeds) and consistency in the sign of the 10m wind speed changes (non shadow areas indicate areas where at least 80% of the CMIP3 models provide changes of the same sign (11/14)).

while the sign of the changes is unclear in the centre and the southwest of France. The dispersion of the models is of the same order of magnitude as the amplitude of the changes all over France. This means that although there is high confidence in the sign of the changes in the southeast and the northwest, the amplitude of the changes remains uncertain.

In AMJJAS, the southern part of France (but the Rhone valley) experiences a decrease of the mean wind speed. This is associated with an increase of the northerly winds all over France. Increase of the northerly winds only leads to a very small increase of the mean wind speed in a very limited area in the Rhone valley, where the complex topography accelerates the wind flows. However, uncertainties are higher than in ONDJFM, implying that the sign and the amplitude of the changes are unclear all over France, except in the Centre (maximum decrease of 4.8%). However, even in the Centre, the dispersion of the models is of the same order of magnitude as the changes. Differences between the 9- and 3-km domains are also weak.

Those results are in agreement with the 10 m wind changes found by Najac *et al*. (2009), with regard to both the sign and the amplitude of the changes.

4.3.2. Changes in the weather type occurrences

The changes in the 10 m winds that have been highlighted previously may be linked to changes in weather type occurrences. The relevance of this approach relies on recent studies which suggested that anthropogenic climate change may manifest itself as a projection onto the preexisting natural modes of variability of the climate system (Corti *et al*., 1999; Stone *et al*., 2001).

As illustrated in Figure 17, multimodel mean changes, reflecting a biased estimator of the response to the anthropogenic forcing, occur in ONDJFM: WT1cold occurrence increases by 8% and WT4cold occurrence by 11%, while WT2cold occurrence decreases by 13% and WT5cold occurrence by 10% (percentages of increase/decrease relative to the frequency of occurrence in the historical simulation). Note that those results agree with previous studies concerning changes in the residence frequency of the climate system in the wintertime North

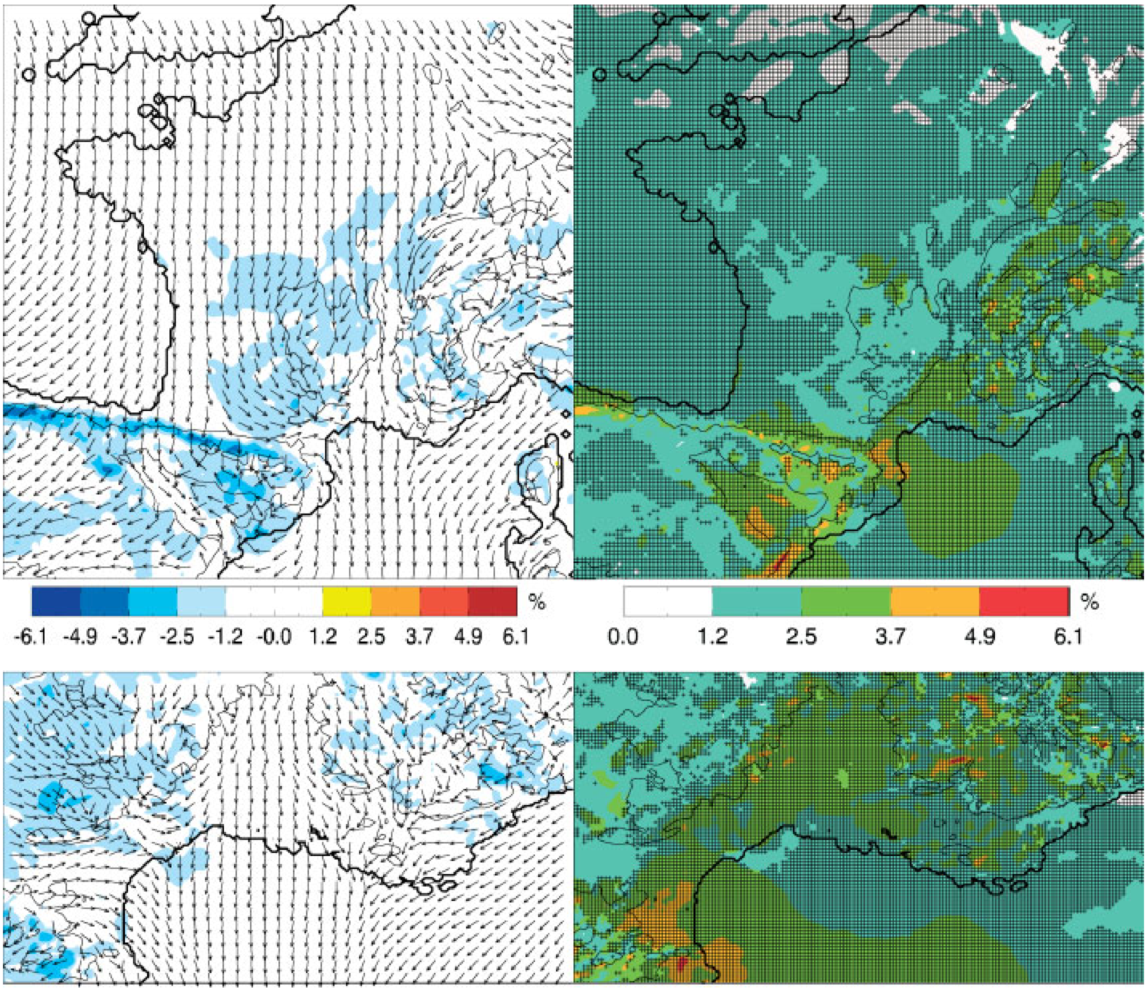

Figure 16. Same as Figure 15, but for AMJJAS.

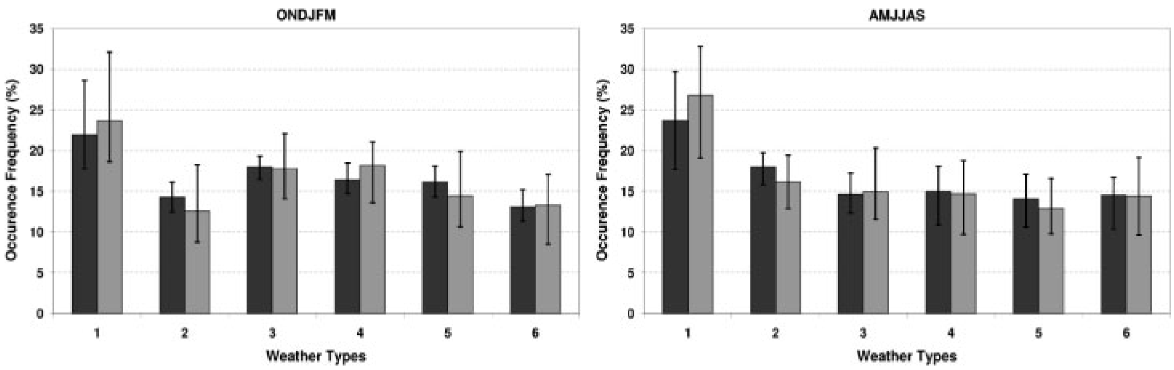

Figure 17. Weather type occurrence frequencies (averaged over all the CMIP3 models) in percent for the cold and warm seasons, for the historical period (dark grey) and 2046–2065 (light-grey). Vertical bars represent the range between the maximum and the minimum values obtained with all models.

Atlantic–European atmospheric circulation regimes (Terray *et al.*, 2004; Stephenson *et al.*, 2006). These 10 m wind changes have amplitude which is usually weaker than the multimodel projection spread, making them hard to detect. Nevertheless, those changes in the weather type occurrences may have additive effects and give rise to larger changes in the wind speed distribution. Indeed, according to Section 4.1 and Figure 3, WT4cold is associated with strong south-westerly winds in northern France, WT1cold with weak anticyclonic winds over France, WT5cold with weak northerly winds in northern France and strong wind events in the Mediterranean area (Mistral and Tramontana), and WT2cold with weak north-easterly winds all over France. As a consequence, in ONDJFM, changes in the weather type occurrence are expected to lead to a decrease of the wind speed in the Mediterranean area and an increase in north-western France. This is in good agreement with the 10 m wind speed changes highlighted in Section 4.3.1.

In AMJJAS, WT1warm occurrence increases by 14%, while WT2warm occurrences decrease by 11% and WT5warm occurrences decrease by 9%. According to Section 4.1 and Figure 4, WT1warm is associated with weak anticyclonic winds over France, WT2warm with southerly winds all over France and WT5warm with strong south-westerly winds in northern France. As a result, changes in the weather type occurrences in AMJJAS are expected to lead to a low decrease of the wind speed all over France. This is also in agreement with the 10 m wind speed changes highlighted in Section 4.3.1.

However, Najac *et al*. (2009) showed that changes in the weather type occurrences are only a part of the climate change signal and are not sufficient to explain the whole change in the 10 m winds. Indeed changes in the distribution of the days within the weather types may be as much important. Note that, in our method, those changes are accounted for by changes in the occurrences of the wind classes, which have been defined within the weather types.

5. Conclusion

In this paper we have presented a statistical–dynamical downscaling method to estimate the 10 m wind speed and direction distributions at high spatial resolution. Relatively good agreements between the observed and the reconstructed wind roses were found, justifying the use of the method in studies of the impacts due to future climate change.

The multimodel study of the impact of climate change on the wind resources over France was carried out for the 2046–2065 period with the 1971–2000 period as a reference. Concerning the mean 10 m wind speeds, although there is confidence in the sign of the changes in some areas (increase in the northwest and decrease in the southeast in ONDJFM, decrease in the Centre in AMJJAS), there is a large uncertainty with regard to the amplitude of those changes. Furthermore, the changes that have been highlighted remain low (maximum of 5.8%). Those results are in good agreement with previous studies (Najac *et al*., 2009).

In this work no attempt has been made to constrain the source of uncertainty linked to the climate models. Many possibilities exist such as to weigh the models according to their ability in reproducing the present climate distributions (Tebaldi and Knutti, 2007) or the key physical processes responsible for the spread of future projections (Boé and Terray, 2008). These different options will be explored in future work.

We have also analysed the various sources of errors from the method itself. The main drawbacks of the statistical–dynamical downscaling method are the addition of two sources of errors (errors that originate from the day sampling and errors that originate from the mesoscale simulations) and the assumption that the climate change signal may be entirely captured by changes in the wind class frequency of occurrence. Furthermore, while a sample of 200 days appeared to be satisfactory to represent the 10 m wind speed and direction distributions, the current version of the method is not adapted for extreme wind studies. The main advantage of this method is that it can provide crucial information at the scale of interest for policymakers. Moreover, given the mesoscale simulations, it can be easily applied to a wide range of GCMs for different time periods, which is essential to carry out relevant impact studies.

Acknowledgements

J. Najac PhD grant was partly supported by Electricité de France (EDF). ECMWF ERA-40 data were obtained from the ECMWF data server. The authors are grateful to the Division de la Climatologie (DCLIM) at Météo-France for providing the SQR dataset. We acknowledge the modelling groups, the Program for Climate Model Diagnosis and Intercomparison (PCMDI) and the WCRP's Working Group on Coupled Modelling (WGCM) for their roles in making available the WCRP CMIP3 multimodel dataset. Support of this dataset is provided by the Office of Science, US Department of Energy. Some statistical calculations have been performed with Statpack, developed by P. Terray (IPSL/LOCEAN). We would like to thank J. Payart for her precious help with the MesoNH model.

References

Boé J, Terray L. 2008. Uncertainties in summer evapotranspiration changes over Europe and implications for regional climate change. *Geophysical Research Letters* **35**: L05702, DOI:10.1029/2007GL032417.

Boé J, Terray L, Habets F, Martin E. 2006. A simple statistical-dynamical downscaling scheme based on weather types and conditional resampling. *Journal of Geophysical Research* **111**: D23106, DOI: 10.1029/2005JD006889.

Bogardi I, Matyasovszky I. 1996. Estimating daily wind speed under climate change. *Solar Energy* **57**(3): 239–248.

Cassou C, Terray L, Phillips AS. 2005. Tropical Atlantic influence on European heatwaves. *Journal of Climate* **18**: 2805–2811.

Conil S, Hall A. 2006. Local regimes of atmospheric variability: a case study of Southern California. *Journal of Climate* **19**(17): 4308–4325.

Corti S, Molteni F, Palmer TN. 1999. Signature of recent climate change in frequencies of natural atmospheric circulation regimes. *Nature* **398**: 799–802.

Frey-Buness F, Heimann D, Sausen R. 1995. A statistical-dynamical downscaling procedure for global climate simulations. *Theoretical and Applied Climatolgy* **50**: 117–131.

Giorgi F, Mearns LO. 1991. Approaches to the simulation of regional climate change: a review. *Reviews of Geophysics* **29**(2): 191–216.

Global Wind Energy Council. 2007. *Global Wind 2007 Report*. http://www.gwec.net/fileadmin/documents/test2/gwec-08-update_FINAL.pdf.

Heimann D. 1986. Estimation of regional surface-layer wind-field characteristics using a three-layer mesoscale model. *Beitraege zur Physik der Atmosphaere* **59**: 518–537.

Jiménez PA, González-Rouco JF, Montavez JP, Garciá-Bustamante E, Navarro J. 2008. Climatology of wind patterns in the Northeast of the Iberian Peninsula. *Internation Journal of Climatology*, DOI:10.1002/joc1705.

Lafore JP, Stein J, Asencio N, Bougeault P, Ducrocq V, Duron J, Fischer C, Hereil P, Mascart P, Pinty JP, Redelsperger JL, Richard E, Vila-Guerau de Arellano J. 1998. The Meso-NH Atmospheric Simulation System. Part I: adiabatic formulation and control simulations. *Annales Geophysicae* **16**: 90–109.

Mengelkamp H-T. 1999. Wind climate simulation over complex terrain and wind turbine energy output estimation. *Theoretical and Applied Climatology* **63**: 129–139.

Mengelkamp H-T, Kapitza H, Pfluger U. 1997. Statistical-dynamical downscaling of wind climatologies. *Journal of Wind Engineering and Industrial Aerodynamics* **67&68**: 449–457.

Moisselin JM, Schneider M, Canellas C, Mestre O. 2002. Changements climatiques en France au 20ème siècle. Etude des longues sèries de donnèes homogènèises françaises de prècipitations et tempèratures. *La Meteorologie* **38**: 45–46.

Najac J. 2008. Impacts du changement climatique sur le potentiel éolien en France : une étude de régionalisation. PhD thesis. Université Toulouse III – Paul Sabatier, 227pp.

Najac J, Boè J, Terray L. 2009. A multi-model ensemble approach for assessment of climate change impact on surface winds in France. *Climate Dynamics* **32**(5): 615–634.

Plaut G, Simonnet E. 2001. Large-scale circulation classification, weather regimes, and local climate over France, the Alps and Western Europe. *Climate Research* **17**: 303–324.

Pryor SC, Barthelmie RJ, Kjellström E. 2005a. Potential climate change impact on wind energy resources in northern Europe: analyses using a regional climate model. *Climate Dynamics* **25**: 815–835.

Pryor SC, Schoof JT. 2005. Empirical downscaling of wind speed probability distributions. *Journal of Geophysical Research* **110**: D19109.

Pryor SC, Schoof JT, Barthelmie RJ. 2005b. Climate change impacts on wind speeds and wind energy density in northern Europe: empirical downscaling of multiple AOGCMs. *Climate Research* **29**: 183–198.

Pryor SC, Schoof JT, Barthelmie RJ. 2006. Winds of change?: projections of near-surfacewinds under climate change scenarios. *Geophysical Research Letters* **33**: L11702.

Sailor DJ, Hu T, Li X, Rosen JN. 2000. A neural network approach to local downscaling of GCM output for assessing wind power implications of climate change. *Renewable Energy* **19**: 359–378.

Stein J, Richard E, Lafore JP, Pinty JP, Asencio N, Cosma S. 2000. High-resolution non-hydrostatic simulations of flash-flood episodes with grid-nesting and ice-phase parametrization. *Meteorology and Atmospheric Physics* **72**: 101–110.

Stephenson DB, Pavan V, Collins M, Junge MM, Quadrelli R, and participating CMIP2 modelling groups. 2006. North Atlantic oscillation response to transient greenhouse gas forcing and the impact on european winter climate: a CMIP2 multi-model assessment. *Climate Dynamics* **27**: 401–420.

Stone DA, Weaver AJ, Stouffer RJ. 2001. Projection of climate change onto modes of atmospheric variability. *Journal of Climate* **14**: 3551–3565.

Taylor KE. 2001. Summarizing multiple aspects of model performance in single diagram. *Journal of Geophysical Research* **106**(D7): 7183–7192.

Tebaldi C, Knutti R. 2007. The use of the multimodel ensemble in probabilistic climate projections. *Philosophical Transactions of the Royal Society of London, Series A* **365**: 2053–2075, DOI:10.1098/rsta.2007.2076.

Terray L, Demory ME, Déqué M, Coetlogon G, Maisonnave E. 2004. Simulation of late-twenty-first-century changes in wintertime atmospheric circulation over Europe due to anthropogenic causes. *Journal of Climate* **17**(24): 4630–4635.

Uppala SM, Kallberg PW, Simmons AJ, Andrae U, da Costa Bechtold V, Fiorino M, Gibson JK, Haseler J, Hernandez A, Kelly GA, Li X, Onogi K, Saarinen S, Sokka N, Allan RP, Andersson E, Arpe K, Balmaseda MA, Beljaars ACM, van de Berg L, Bidlot J, Bormann N, Caires S, Chevallier F, Dethof A, Dragosavac M, Fisher M, Fuentes M, Hagemann S, Holm E, Hoskins BJ, Isaksen L, Janssen PAEM, Jenne R, McNally AP, Mahfouf J-F, Morcrette J-J, Rayner NA, Saunders RW, Simon P, Sterl A, Trenberth KE, Untch A, Vasiljevic D, Viterbo P, Woollen J. 2005. The ERA-40 re-analysis. *Quarterly Journal of the Royal Meteorological Society* **131**: 2961–3012.

Wilby RL, Charles SP, Zorita E, Timbal B, Whetton P, Mearns LO. 2004. *Guidelines for Use of Climate Scenarios Developed from Statistical Downscaling Methods*. Data Distribution Centre of the Intergovernmental Panel on Climate Change.

Wippermann F, Gross G. 1981. On the construction of orographically influenced wind roses for given distribution of the large-scale wind. *Beitraege zur Physik der Atmosphaere* **54**: 492–501.

